International Journal of Solids and Structures 41 (2004) 4179–4196

INTERNATIONAL JOURNAL OF SOLIDS and STRUCTURES

www.elsevier.com/locate/ijsolstr

Electro-elastic analysis of a bimaterial piezoelectric wedge with an interface crack under antiplane concentrated forces and inplane surface charges

Ching-Hwei Chue *, Thomas Jin-Chee Liu

Department of Mechanical Engineering, National Cheng Kung University, 70101 Tainan, Taiwan, ROC

Received 8 July 2003; received in revised form 14 January 2004
Available online 27 March 2004

Abstract

The antiplane electro-elastic field for a bimaterial piezoelectric wedge with an interface crack subjected to a pair of concentrated forces and surface charges is studied in this paper. Based on the Mellin transform and the singular integral equation, the stress, strain, electric displacement, electric field intensity factors at both crack tips are derived analytically. These parameters can be applied to examine the fracture behavior of the interface crack. The results are validated when the problem is reduced to some simple cases studied in previous open literatures.

Keywords: Bimaterial piezoelectric wedge; Interface crack; Antiplane deformation; Mellin transform; Singular integral equation; Intensity factors

1. Introduction

Due to the capability of the transfer between mechanical and electric energy, piezoelectric materials are widely used in smart structures, sensors, and actuators. These structures usually involve wedge shape structures at some local regions, where the geometry and material are discontinuous. The singular stress field may occur at the wedge apex where the crack initiates.

Antiplane deformation problems of isotropic and anisotropic elastic wedges have been studied in the past (Erdogan and Gupta, 1975; Ma and Hour, 1989; Kargarnovin et al., 1997; Shahani, 1999; Shahani and Adibnazari, 2000; Shahani, 2001; Chue and Liu, 2001). Xu and Rajapakse (2000) and Chue and Chen (2002, 2003) solved the stress singularities for a multi-material wedge bonded by composites, electrodes, and piezoelectric materials. Wei et al. (2002) and Chue et al. (2003) used the Mellin transform to obtain the antiplane electro-elastic field and intensity factors of the single-material and bimaterial piezoelectric wedges subjected to a pair of concentrated forces and free charges.

* Corresponding author. Tel.: +886-6-2757575x62165; fax: +886-6-2352973.
E-mail address: chchue@mail.ncku.edu.tw (C.-H. Chue).

0020-7683/$ - see front matter
doi:10.1016/j.ijsolstr.2004.02.044

The existence of cracks in bimaterial wedges cannot be completely avoided. In reality, cracks may occur on the interface of two bonded wedges due to debonding. Erdogan and Gupta (1975) used the Mellin transform and the singular integral equation to study the interface crack in a bimaterial elastic wedge under antiplane loadings applied at crack faces. Shahani and Adibnazari (2000) studied similar bimaterial elastic wedges under a pair of concentrated antiplane forces applied at wedge edges. In their paper, the problems of bonded wedges with an interface crack and the related cases were studied. A screw dislocation $f(r)$ was proposed to solve the stress components, singularity orders, and intensity factors. More recently, Shahani (2001) examined the behavior of $f(r)$ when one of the interface crack tips approaches the wedge apex.

In this paper, we study the antiplane deformation of the bimaterial piezoelectric wedge with an interface crack subjected to a pair of antiplane concentrated forces and inplane electric surface charges. The intensity factors of stress, strain, electric displacement and electric fields at crack tips are derived analytically.

Early in 1990, Pak studied the crack behavior in a piezoelectric material and considered the crack to be impermeable; filled with a vacuum or a nonconducting gas. Zhang et al. (2002) and Zhang and Tong (1996) theoretically studied the electrically impermeable and permeable boundary conditions. In addition, the electric boundary conditions, in particular, for a mode III crack in a piezoelectric material were discussed in detail by Zhang and Tong (1996). As described in the review article (Zhang et al., 2002), the electrically impermeable and permeable boundary conditions are two extreme approximations for an electrically insulated crack. A recent experimental work (Schneider et al., 2003) indicates that the permeable boundary conditions are more reasonable than the impermeable boundary conditions.

However, due to the mathematical difficulties posed by applying the Mellin transform to the piezoelectric wedge problem with an interface crack, the crack is assumed to be impermeable for this study.

2. Problem statements and basic formulations

The structure shown in Fig. 1 is composed of two bonded piezoelectric wedges with same wedge angle α and an interface crack AB located on the common edge ($\theta = 0°$) between $r = a$ and $r = b$. The crack surfaces are traction-free and impermeable (Pak, 1990). A pair of longitudinal shearing forces F and another two inplane surface charges Q are applied on the edges $r = h$. Because the wedge has an infinite length along the z-axis, this problem becomes a generalized plane deformation problem. Since the piezoelectric

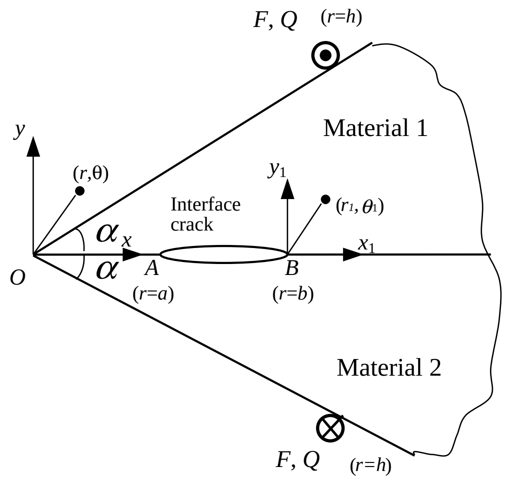

Fig. 1. Configuration of a bimaterial piezoelectric wedge with an interface crack.

materials are polarized in the z-direction, only the antiplane elastic field coupled with the inplane electric field is considered in the analysis. The field quantities include the shear stresses $(\sigma_{rz}, \sigma_{\theta z})$, shear strains $(\gamma_{rz}, \gamma_{\theta z})$, elastic deformation (w), electric displacements (D_r, D_θ), electric fields (E_r, E_θ) and electric potential (ϕ). They are functions of r and θ only.

The constitutive equations of this antiplane problem can be written as follows

$$\begin{bmatrix} \sigma_{\theta z}^{(i)} \\ \sigma_{rz}^{(i)} \\ D_r^{(i)} \\ D_\theta^{(i)} \end{bmatrix} = \begin{bmatrix} c_{44}^{(i)} & 0 & 0 & -e_{15}^{(i)} \\ 0 & c_{44}^{(i)} & -e_{15}^{(i)} & 0 \\ 0 & e_{15}^{(i)} & \varepsilon_{11}^{(i)} & 0 \\ e_{15}^{(i)} & 0 & 0 & \varepsilon_{11}^{(i)} \end{bmatrix} \begin{bmatrix} \gamma_{\theta z}^{(i)} \\ \gamma_{rz}^{(i)} \\ E_r^{(i)} \\ E_\theta^{(i)} \end{bmatrix}, \quad i = 1, 2 \tag{1}$$

where the material constants c_{44}, ε_{11}, and e_{15} are the elastic stiffness constant, dielectric constant, and piezoelectric constant, respectively. The superscript i denotes materials 1 and 2. In the absence of body forces and free charges, the equilibrium equation in terms of stresses and the Maxwell equation for electric displacements are

$$\frac{\partial}{\partial r}(r\sigma_{rz}^{(i)}) + \frac{\partial}{\partial \theta}(\sigma_{\theta z}^{(i)}) = 0 \tag{2}$$

$$\frac{\partial}{\partial r}(rD_r^{(i)}) + \frac{\partial}{\partial \theta}(D_\theta^{(i)}) = 0 \tag{3}$$

respectively. The shear strain–displacement relations are

$$\gamma_{\theta z}^{(i)} = \frac{1}{r}\frac{\partial w^{(i)}}{\partial \theta} \tag{4a}$$

$$\gamma_{rz}^{(i)} = \frac{\partial w^{(i)}}{\partial r} \tag{4b}$$

where w is the displacement in the z-direction. The electric field components are written in terms of the inplane electric potential ϕ as

$$E_r^{(i)} = -\frac{\partial \phi^{(i)}}{\partial r} \tag{5a}$$

$$E_\theta^{(i)} = -\frac{1}{r}\frac{\partial \phi^{(i)}}{\partial \theta} \tag{5b}$$

Substituting (4) and (5) into (1) and using (2) and (3), the governing equations for antiplane displacement w and inplane electric potential ϕ are obtained as

$$c_{44}^{(i)}\nabla^2 w^{(i)} + e_{15}^{(i)}\nabla^2\phi^{(i)} = 0 \tag{6a}$$

$$e_{15}^{(i)}\nabla^2 w^{(i)} - \varepsilon_{11}^{(i)}\nabla^2\phi^{(i)} = 0 \tag{6b}$$

where ∇^2 is two-dimensional Laplace operator in (r, θ) as

$$\nabla^2 = \frac{\partial^2}{\partial r^2} + \frac{1}{r}\frac{\partial}{\partial r} + \frac{1}{r^2}\frac{\partial^2}{\partial \theta^2} \tag{7}$$

Solving for w and ϕ from (6), the results are

$$\nabla^2 w^{(i)} = 0 \tag{8}$$

$$\nabla^2\phi^{(i)} = 0 \tag{9}$$

The stresses and electric displacements can be related to w and ϕ by the following relations

$$\sigma_{\theta z}^{(i)} = \frac{1}{r}\left[c_{44}^{(i)}\frac{\partial w^{(i)}}{\partial\theta} + e_{15}^{(i)}\frac{\partial\phi^{(i)}}{\partial\theta}\right] \tag{10a}$$

$$\sigma_{rz}^{(i)} = c_{44}^{(i)}\frac{\partial w^{(i)}}{\partial r} + e_{15}^{(i)}\frac{\partial\phi^{(i)}}{\partial r} \tag{10b}$$

$$D_r^{(i)} = e_{15}^{(i)}\frac{\partial w^{(i)}}{\partial r} - \varepsilon_{11}^{(i)}\frac{\partial\phi^{(i)}}{\partial r} \tag{11a}$$

$$D_\theta^{(i)} = \frac{1}{r}\left[e_{15}^{(i)}\frac{\partial w^{(i)}}{\partial\theta} - \varepsilon_{11}^{(i)}\frac{\partial\phi^{(i)}}{\partial\theta}\right] \tag{11b}$$

The boundary conditions on the edges of the wedge ($\theta = \pm\alpha$) are as follows

$$\sigma_{\theta z}^{(1)}(r,\alpha) = F\delta(r-h) \tag{12a}$$

$$\sigma_{\theta z}^{(2)}(r,-\alpha) = F\delta(r-h) \tag{12b}$$

$$D_\theta^{(1)}(r,\alpha) = Q\delta(r-h) \tag{12c}$$

$$D_\theta^{(2)}(r,-\alpha) = Q\delta(r-h) \tag{12d}$$

where δ is the Dirac–Delta function. Without loss of generality, the distance h satisfies the relation $a \leqslant b \leqslant h$. The continuity conditions along the bonded interface ($\theta = 0°$) and the interface crack are

$$w^{(1)}(r,0) = w^{(2)}(r,0), \quad \phi^{(1)}(r,0) = \phi^{(2)}(r,0), \qquad 0 \leqslant r \leqslant a, \ \ b \leqslant r < \infty \tag{13}$$

$$\sigma_{\theta z}^{(1)}(r,0) = \sigma_{\theta z}^{(2)}(r,0), \quad D_\theta^{(1)}(r,0) = D_\theta^{(2)}(r,0), \qquad 0 \leqslant r < \infty \tag{14}$$

On the crack surfaces, the traction-free and surface charge-free conditions are

$$\sigma_{\theta z}^{(1)}(r,0) = \sigma_{\theta z}^{(2)}(r,0) = 0, \quad D_\theta^{(1)}(r,0) = D_\theta^{(2)}(r,0) = 0, \qquad a \leqslant r \leqslant b \tag{15}$$

It has been assumed that the crack is impermeable in (15).

3. Solutions

3.1. Antiplane displacements and inplane electric potentials

The Mellin transform method has been widely used to solve the physical problems when the governing equations are expressed in polar coordinates. For a given function, $F(r,\theta)$, the Mellin transform and its inversion are defined as (Sneddon, 1972)

$$\overline{F}(p,\theta) = \int_0^\infty F(r,\theta)r^{p-1}\,\mathrm{d}r \tag{16}$$

$$F(r,\theta) = \frac{1}{2\pi\mathrm{i}}\int_{c-\mathrm{i}\infty}^{c+\mathrm{i}\infty} \overline{F}(p,\theta)r^{-p}\,\mathrm{d}p \tag{17}$$

where p is a complex transform parameter and the bar over the function F denotes the transformed quantity. The constant $\mathrm{Re}[p] = c$ defines the path of integration. Applying the Mellin transform with integration by parts on (8), gives

$$\frac{\mathrm{d}^2\overline{w}^{(i)}}{\mathrm{d}\theta^2} + p^2\overline{w}^{(i)} = 0 \tag{18}$$

provided that (Sneddon, 1972)

$$\left[r^{p+1}\frac{\partial w^{(i)}}{\partial r} - pr^p w^{(i)}\right]_0^\infty = 0 \tag{19}$$

The solutions of (18) for materials 1 and 2 are

$$\overline{w}^{(1)} = C_1(p)\cos p\theta + C_2(p)\sin p\theta \tag{20}$$

$$\overline{w}^{(2)} = C_5(p)\cos p\theta + C_6(p)\sin p\theta \tag{21}$$

where C_i $(i = 1, 2, 5, 6)$ are unknown functions of p. In a similar manner, the transformed electric potentials may be obtained as

$$\overline{\phi}^{(1)} = C_3(p)\cos p\theta + C_4(p)\sin p\theta \tag{22}$$

$$\overline{\phi}^{(2)} = C_7(p)\cos p\theta + C_8(p)\sin p\theta \tag{23}$$

The functions C_1, C_2, C_3, C_4, C_5, C_6, C_7 and C_8 can be deduced from (12)–(15).

From (13) and (15), an unknown function $f(r)$ is defined as (Erdogan and Biricikoglu, 1973)

$$f(r) = \frac{\partial}{\partial r}\left[w^{(1)}(r, +0) - w^{(2)}(r, -0)\right] \tag{24}$$

Substituting Eq. (13) into Eq. (24), yields

$$f(r) = 0, \quad 0 \leqslant r \leqslant a, \quad b \leqslant r < \infty \tag{25}$$

The unknown function $f(r)$ is nonzero in the interval $a \leqslant r \leqslant b$. Also, the single-valuedness condition of displacements requires that

$$\int_a^b f(r)\,\mathrm{d}r = 0 \tag{26}$$

In a similar manner, another unknown function $g(r)$ for electric potential (Chen and Worswick, 2000) is defined as

$$g(r) = \frac{\partial}{\partial r}\left[\phi^{(1)}(r, +0) - \phi^{(2)}(r, -0)\right] \tag{27}$$

with

$$g(r) = 0, \quad 0 \leqslant r \leqslant a, \quad b \leqslant r < \infty \tag{28}$$

$$\int_a^b g(r)\,\mathrm{d}r = 0 \tag{29}$$

Substituting (10) and (11) into the boundary conditions (12) and then applying the Mellin transform on both sides, result in

$$c_{44}^{(1)}\frac{\partial\overline{w}^{(1)}(p,\alpha)}{\partial\theta}+e_{15}^{(1)}\frac{\partial\overline{\phi}^{(1)}(p,\alpha)}{\partial\theta}=Fh^p \tag{30a}$$

$$c_{44}^{(2)}\frac{\partial\overline{w}^{(2)}(p,-\alpha)}{\partial\theta}+e_{15}^{(2)}\frac{\partial\overline{\phi}^{(2)}(p,-\alpha)}{\partial\theta}=Fh^p \tag{30b}$$

$$e_{15}^{(1)}\frac{\partial\overline{w}^{(1)}(p,\alpha)}{\partial\theta}-\varepsilon_{11}^{(1)}\frac{\partial\overline{\phi}^{(1)}(p,\alpha)}{\partial\theta}=Qh^p \tag{31a}$$

$$e_{15}^{(2)}\frac{\partial\overline{w}^{(2)}(p,-\alpha)}{\partial\theta}-\varepsilon_{11}^{(2)}\frac{\partial\overline{\phi}^{(2)}(p,-\alpha)}{\partial\theta}=Qh^p \tag{31b}$$

Substituting (10) and (11) into continuity conditions (14) and then applying the Mellin transform, lead to

$$c_{44}^{(1)}\frac{\partial\overline{w}^{(1)}(p,0)}{\partial\theta}+e_{15}^{(1)}\frac{\partial\overline{\phi}^{(1)}(p,0)}{\partial\theta}=c_{44}^{(2)}\frac{\partial\overline{w}^{(2)}(p,0)}{\partial\theta}+e_{15}^{(2)}\frac{\partial\overline{\phi}^{(2)}(p,0)}{\partial\theta} \tag{32a}$$

$$e_{15}^{(1)}\frac{\partial\overline{w}^{(1)}(p,0)}{\partial\theta}-\varepsilon_{11}^{(1)}\frac{\partial\overline{\phi}^{(1)}(p,0)}{\partial\theta}=e_{15}^{(2)}\frac{\partial\overline{w}^{(2)}(p,0)}{\partial\theta}-\varepsilon_{11}^{(2)}\frac{\partial\overline{\phi}^{(2)}(p,0)}{\partial\theta} \tag{32b}$$

In addition, applying the Mellin transform on (24) and (27) respectively, the results become

$$\int_a^b f(v)v^p\,\mathrm{d}v=-p(C_1-C_5) \tag{33a}$$

$$\int_a^b g(v)v^p\,\mathrm{d}v=-p(C_3-C_7) \tag{33b}$$

Substituting (20)–(23) into (30)–(32) and using (33), eight simultaneous equations are obtained for solving the eight unknowns C_1–C_8. Since the intensity factors are the focus of this paper, we consider the electro-elastic field of material 1 only. The solutions of C_1, C_2, C_3 and C_4 are

$$C_1=\frac{\left(\int_a^b g(v)v^p\,\mathrm{d}v\right)f_1-\left(\int_a^b f(v)v^p\,\mathrm{d}v\right)f_2}{pf_3} \tag{34a}$$

$$C_2=\frac{h^pf_7f_3-f_4\sin(p\alpha)\left[-f_1\left(\int_a^b g(v)v^p\,\mathrm{d}v\right)+f_2\left(\int_a^b f(v)v^p\,\mathrm{d}v\right)\right]}{p\cos(p\alpha)f_3f_4} \tag{34b}$$

$$C_3=\frac{\left(\int_a^b f(v)v^p\,\mathrm{d}v\right)f_5-\left(\int_a^b g(v)v^p\,\mathrm{d}v\right)f_6}{pf_3} \tag{34c}$$

$$C_4=\frac{h^pf_8f_3-f_4\sin(p\alpha)\left[-f_5\left(\int_a^b f(v)v^p\,\mathrm{d}v\right)+f_6\left(\int_a^b g(v)v^p\,\mathrm{d}v\right)\right]}{p\cos(p\alpha)f_3f_4} \tag{34d}$$

where

$$f_1=-e_{15}^{(2)}\varepsilon_{11}^{(1)}+e_{15}^{(1)}\varepsilon_{11}^{(2)} \tag{35a}$$

$$f_2 = e_{15}^{(1)} e_{15}^{(2)} + e_{15}^{(2)^2} + c_{44}^{(2)} \left[\varepsilon_{11}^{(1)} + \varepsilon_{11}^{(2)} \right] \tag{35b}$$

$$f_3 = e_{15}^{(1)^2} + 2e_{15}^{(1)} e_{15}^{(2)} + e_{15}^{(2)^2} + \left[c_{44}^{(1)} + c_{44}^{(2)} \right] \left[\varepsilon_{11}^{(1)} + \varepsilon_{11}^{(2)} \right] \tag{35c}$$

$$f_4 = e_{15}^{(1)^2} + c_{44}^{(1)} \varepsilon_{11}^{(1)} \tag{35d}$$

$$f_5 = -c_{44}^{(2)} e_{15}^{(1)} + c_{44}^{(1)} e_{15}^{(2)} \tag{35e}$$

$$f_6 = e_{15}^{(1)} e_{15}^{(2)} + e_{15}^{(2)^2} + \varepsilon_{11}^{(2)} \left[c_{44}^{(1)} + c_{44}^{(2)} \right] \tag{35f}$$

$$f_7 = e_{15}^{(1)} Q + \varepsilon_{11}^{(1)} F \tag{35g}$$

$$f_8 = e_{15}^{(1)} F - c_{44}^{(1)} Q \tag{35h}$$

Substituting (34) back into (20) and (21), and applying inverse Mellin transform on $\overline{w}^{(1)}$ and $\overline{\phi}^{(1)}$, the displacement $w^{(1)}$ and the electric potential $\phi^{(1)}$ in material 1 are given by

$$\begin{aligned} w^{(1)} = {} & \left(\frac{f_7}{f_4}\right) \frac{1}{2\pi \mathrm{i}} \int_{c-\mathrm{i}\infty}^{c+\mathrm{i}\infty} \left[\frac{\sin(p\theta)}{p\cos(p\alpha)} \right] \left(\frac{h}{r}\right)^p \mathrm{d}p - \left(\frac{f_2}{f_3}\right) \frac{1}{2\pi \mathrm{i}} \int_{c-\mathrm{i}\infty}^{c+\mathrm{i}\infty} \left[\frac{\cos(p\theta)}{p} + \frac{\sin(p\alpha)\sin(p\theta)}{p\cos(p\alpha)} \right] \\ & \times \left[\int_a^b f(v) \left(\frac{v}{r}\right)^p \mathrm{d}v \right] \mathrm{d}p + \left(\frac{f_1}{f_3}\right) \frac{1}{2\pi \mathrm{i}} \int_{c-\mathrm{i}\infty}^{c+\mathrm{i}\infty} \left[\frac{\cos(p\theta)}{p} + \frac{\sin(p\alpha)\sin(p\theta)}{p\cos(p\alpha)} \right] \left[\int_a^b g(v) \left(\frac{v}{r}\right)^p \mathrm{d}v \right] \mathrm{d}p \end{aligned} \tag{36}$$

$$\begin{aligned} \phi^{(1)} = {} & \left(\frac{f_8}{f_4}\right) \frac{1}{2\pi \mathrm{i}} \int_{c-\mathrm{i}\infty}^{c+\mathrm{i}\infty} \left[\frac{\sin(p\theta)}{p\cos(p\alpha)} \right] \left(\frac{h}{r}\right)^p \mathrm{d}p + \left(\frac{f_5}{f_3}\right) \frac{1}{2\pi \mathrm{i}} \int_{c-\mathrm{i}\infty}^{c+\mathrm{i}\infty} \left[\frac{\cos(p\theta)}{p} + \frac{\sin(p\alpha)\sin(p\theta)}{p\cos(p\alpha)} \right] \\ & \times \left[\int_a^b f(v) \left(\frac{v}{r}\right)^p \mathrm{d}v \right] \mathrm{d}p - \left(\frac{f_6}{f_3}\right) \frac{1}{2\pi \mathrm{i}} \int_{c-\mathrm{i}\infty}^{c+\mathrm{i}\infty} \left[\frac{\cos(p\theta)}{p} + \frac{\sin(p\alpha)\sin(p\theta)}{p\cos(p\alpha)} \right] \left[\int_a^b g(v) \left(\frac{v}{r}\right)^p \mathrm{d}v \right] \mathrm{d}p \end{aligned} \tag{37}$$

The residue theorem and appropriate path of integration will be applied to solve for the integrals of (36) and (37). Looking at the first integral of (36) and (37), the poles p_n are computed from $\cos(p\alpha) = 0$ as follows

$$p_{\pm n} = \pm \frac{2n-1}{2\alpha} \pi, \quad n = 1, 2, \ldots, \infty \tag{38}$$

The constant $\mathrm{Re}[p] = c$ is chosen to satisfy the limiting conditions (19). It requires that the following conditions should be satisfied:

$$r \leqslant h, \quad p_{-n} < 0, \quad c > \mathrm{Re}[p_{-n}] \tag{39}$$

$$r \geqslant h, \quad p_n > 0, \quad c < \mathrm{Re}[p_n] \tag{40}$$

The constant c is chosen in the interval $p_{-1} < c < p_1$.

Although (36) and (37) are valid for $0 \leqslant r \leqslant \infty$, only the region $a \leqslant r \leqslant b$ is considered. Using the residue theorem, the first integral of (36) and (37) for $r \leqslant h$ are obtained as follows

$$\frac{1}{2\pi i}\int_{c-i\infty}^{c+i\infty}\left[\frac{\sin(p\theta)}{p\cos(p\alpha)}\right]\left(\frac{h}{r}\right)^{p}dp=\left(\frac{-2}{\pi}\right)\sum_{n=1}^{\infty}\frac{(-1)^{n}}{2n-1}\left(\frac{r}{h}\right)^{p_n}\sin(p_n\theta),\quad r\leqslant h \tag{41}$$

For the region $a\leqslant r\leqslant b$, the second integral of (36) and (37) can be divided into two integral regions $[a,r]$ and $[r,b]$ (Shahani and Adibnazari, 2000) so that the residue theorem can be applied. Using the residue theorem, the result is

$$\begin{aligned}&\frac{1}{2\pi i}\int_{c-i\infty}^{c+i\infty}\left[\frac{\cos(p\theta)}{p}+\frac{\sin(p\alpha)\sin(p\theta)}{p\cos(p\alpha)}\right]\left[\int_a^b f(v)\left(\frac{v}{r}\right)^{p}dv\right]dp\\&=\frac{1}{2\pi i}\int_{c-i\infty}^{c+i\infty}\left[\frac{\cos(p\theta)}{p}+\frac{\sin(p\alpha)\sin(p\theta)}{p\cos(p\alpha)}\right]\left[\int_a^r f(v)\left(\frac{v}{r}\right)^{p}dv+\int_r^b f(v)\left(\frac{v}{r}\right)^{p}dv\right]dp\\&=\sum_{n=1}^{\infty}\frac{\left[\int_a^r f(v)\left(\frac{v}{r}\right)^{p_n}dv-\int_r^b f(v)\left(\frac{v}{r}\right)^{-p_n}dv\right]\cos(p_n\alpha-p_n\theta)}{p_n\alpha\sin(p_n\alpha)},\quad a\leqslant r\leqslant b\end{aligned} \tag{42}$$

In a similar manner, the third integral of (36) and (37) can be solved as

$$\begin{aligned}&\frac{1}{2\pi i}\int_{c-i\infty}^{c+i\infty}\left[\frac{\cos(p\theta)}{p}+\frac{\sin(p\alpha)\sin(p\theta)}{p\cos(p\alpha)}\right]\left[\int_a^b g(v)\left(\frac{v}{r}\right)^{p}dv\right]dp\\&=\sum_{n=1}^{\infty}\frac{\left[\int_a^r g(v)\left(\frac{v}{r}\right)^{p_n}dv-\int_r^b g(v)\left(\frac{v}{r}\right)^{-p_n}dv\right]\cos(p_n\alpha-p_n\theta)}{p_n\alpha\sin(p_n\alpha)},\quad a\leqslant r\leqslant b\end{aligned} \tag{43}$$

Substituting (41)–(43) into (36) and (37), the antiplane displacement and the inplane electric potential in the region $a\leqslant r\leqslant b$ of material 1 can be obtained as follows

$$\begin{aligned}w^{(1)}=&\left(\frac{f_7}{f_4}\right)\left(\frac{-2}{\pi}\right)\sum_{n=1}^{\infty}\frac{(-1)^{n}}{2n-1}\left(\frac{r}{h}\right)^{p_n}\sin(p_n\theta)-\\&\left(\frac{f_2}{f_3}\right)\sum_{n=1}^{\infty}\frac{\left[\int_a^r f(v)\left(\frac{v}{r}\right)^{p_n}dv-\int_r^b f(v)\left(\frac{v}{r}\right)^{-p_n}dv\right]\cos(p_n\alpha-p_n\theta)}{p_n\alpha\sin(p_n\alpha)}+\\&\left(\frac{f_1}{f_3}\right)\sum_{n=1}^{\infty}\frac{\left[\int_a^r g(v)\left(\frac{v}{r}\right)^{p_n}dv-\int_r^b g(v)\left(\frac{v}{r}\right)^{-p_n}dv\right]\cos(p_n\alpha-p_n\theta)}{p_n\alpha\sin(p_n\alpha)},\quad a\leqslant r\leqslant b\end{aligned} \tag{44}$$

$$\begin{aligned}\phi^{(1)}=&\left(\frac{f_8}{f_4}\right)\left(\frac{-2}{\pi}\right)\sum_{n=1}^{\infty}\frac{(-1)^{n}}{2n-1}\left(\frac{r}{h}\right)^{p_n}\sin(p_n\theta)+\\&\left(\frac{f_5}{f_3}\right)\sum_{n=1}^{\infty}\frac{\left[\int_a^r f(v)\left(\frac{v}{r}\right)^{p_n}dv-\int_r^b f(v)\left(\frac{v}{r}\right)^{-p_n}dv\right]\cos(p_n\alpha-p_n\theta)}{p_n\alpha\sin(p_n\alpha)}-\\&\left(\frac{f_6}{f_3}\right)\sum_{n=1}^{\infty}\frac{\left[\int_a^r g(v)\left(\frac{v}{r}\right)^{p_n}dv-\int_r^b g(v)\left(\frac{v}{r}\right)^{-p_n}dv\right]\cos(p_n\alpha-p_n\theta)}{p_n\alpha\sin(p_n\alpha)},\quad a\leqslant r\leqslant b\end{aligned} \tag{45}$$

Note that the functions $f(r)$ and $g(r)$ are still unknown and will be solved in the next section.

3.2. The functions $f(r)$ and $g(r)$

In this section, functions $f(r)$ and $g(r)$ are solved in the region $a \leqslant r \leqslant b$. Substituting (44) and (45) into (10)–(11) and using (15), we obtain the following two equations:

$$c_{44}^{(1)}[A_1 - (A_2 - A_3) + (A_4 - A_5)] + e_{15}^{(1)}\left[A_6 + \frac{f_5}{f_2}(A_2 - A_3) - \frac{f_6}{f_1}(A_4 - A_5)\right] = 0 \tag{46a}$$

$$e_{15}^{(1)}[A_1 - (A_2 - A_3) + (A_4 - A_5)] - \varepsilon_{11}^{(1)}\left[A_6 + \frac{f_5}{f_2}(A_2 - A_3) - \frac{f_6}{f_1}(A_4 - A_5)\right] = 0 \tag{46b}$$

or

$$A_1 - (A_2 - A_3) + (A_4 - A_5) = 0 \tag{47a}$$

$$A_6 + \frac{f_5}{f_2}(A_2 - A_3) - \frac{f_6}{f_1}(A_4 - A_5) = 0 \tag{47b}$$

where

$$A_1 = \left(\frac{-f_7}{f_4}\right)\left(\frac{2}{\pi}\right)\sum_{n=1}^{\infty}\frac{(-1)^n}{2n-1}\left(\frac{r}{h}\right)^{p_n} p_n \tag{48a}$$

$$A_2 = \left(\frac{f_2}{\alpha f_3}\right)\sum_{n=1}^{\infty}\int_a^r f(v)\left(\frac{v}{r}\right)^{p_n}\mathrm{d}v \tag{48b}$$

$$A_3 = \left(\frac{f_2}{\alpha f_3}\right)\sum_{n=1}^{\infty}\int_r^b f(v)\left(\frac{v}{r}\right)^{-p_n}\mathrm{d}v \tag{48c}$$

$$A_4 = \left(\frac{f_1}{\alpha f_3}\right)\sum_{n=1}^{\infty}\int_a^r g(v)\left(\frac{v}{r}\right)^{p_n}\mathrm{d}v \tag{48d}$$

$$A_5 = \left(\frac{f_1}{\alpha f_3}\right)\sum_{n=1}^{\infty}\int_r^b g(v)\left(\frac{v}{r}\right)^{-p_n}\mathrm{d}v \tag{48e}$$

$$A_6 = \frac{f_8}{f_7}A_1 \tag{48f}$$

The solutions of (47) are

$$\left(\frac{f_6}{f_1} + \frac{f_8}{f_7}\right)A_1 = \left(\frac{-f_5}{f_2} + \frac{f_6}{f_1}\right)(A_2 - A_3) \tag{49}$$

$$\left(\frac{f_5}{f_2} + \frac{f_8}{f_7}\right)A_1 = \left(\frac{-f_5}{f_2} + \frac{f_6}{f_1}\right)(A_4 - A_5) \tag{50}$$

Changing all series of (48) to begin with $n = 0$ and substituting them into (49) and (50), the results are

$$\frac{\left(\frac{f_6}{f_1} + \frac{f_8}{f_7}\right)\left(\frac{f_7}{f_4}\right)}{\left(\frac{f_6}{f_1} - \frac{f_5}{f_2}\right)\left(\frac{f_2}{f_3}\right)}\left(\frac{r}{h}\right)^{\frac{\pi}{2\alpha}}\sum_{n=0}^{\infty}(-1)^n\left(\frac{r}{h}\right)^{\frac{n\pi}{\alpha}} = \int_a^r\left(\frac{v}{r}\right)^{\frac{\pi}{2\alpha}}\sum_{n=0}^{\infty}\left(\frac{v}{r}\right)^{\frac{n\pi}{\alpha}}f(v)\,\mathrm{d}v - \int_r^b\left(\frac{r}{v}\right)^{\frac{\pi}{2\alpha}}\sum_{n=0}^{\infty}\left(\frac{r}{v}\right)^{\frac{n\pi}{\alpha}}f(v)\,\mathrm{d}v \tag{51}$$

$$\frac{\left(\frac{f_5}{f_2}+\frac{f_8}{f_7}\right)\left(\frac{f_9}{f_4}\right)}{\left(\frac{f_6}{f_1}-\frac{f_5}{f_2}\right)\left(\frac{f_1}{f_3}\right)}\left(\frac{r}{h}\right)^{\frac{\pi}{2\alpha}}\sum_{n=0}^{\infty}(-1)^n\left(\frac{r}{h}\right)^{\frac{n\pi}{\alpha}}=\int_a^r\left(\frac{v}{r}\right)^{\frac{\pi}{2\alpha}}\sum_{n=0}^{\infty}\left(\frac{v}{r}\right)^{\frac{n\pi}{\alpha}}g(v)\,\mathrm{d}v-\int_r^b\left(\frac{r}{v}\right)^{\frac{\pi}{2\alpha}}\sum_{n=0}^{\infty}\left(\frac{r}{v}\right)^{\frac{n\pi}{\alpha}}g(v)\,\mathrm{d}v \quad (52)$$

The following mathematical derivations are similar to those used by Shahani and Adibnazari (2000). Eq. (51) can be reduced to the following form

$$\int_c^d \frac{\phi(t)}{t-x}\,\mathrm{d}t=-\zeta\frac{\left(\frac{f_6}{f_1}+\frac{f_8}{f_7}\right)\left(\frac{f_7}{f_4}\right)}{\left(\frac{f_6}{f_1}-\frac{f_5}{f_2}\right)\left(\frac{f_2}{f_3}\right)}\frac{\sqrt{e}}{e+x};\quad c\leqslant x\leqslant d \quad (53)$$

where

$$\zeta=\pi/\alpha,\quad t=v^{\zeta},\quad x=r^{\zeta},\quad c=a^{\zeta},\quad d=b^{\zeta},\quad e=h^{\zeta} \quad (54a)$$

$$\phi(t)=t^{(1/\zeta-1/2)}f(t^{1/\zeta}) \quad (54b)$$

From the definition in (54), condition (26) becomes

$$\int_c^d \frac{\phi(t)}{t^{1/2}}\,\mathrm{d}t=0 \quad (55)$$

The solution of (53) for $\phi(x)$ is (Muskhelishvili, 1953; Shahani and Adibnazari, 2000)

$$\phi(x)=[(x-c)(d-x)]^{-1/2}\left[B-\frac{1}{\pi^2}\int_c^d[(t-c)(d-t)]^{1/2}\frac{P(t)}{t-x}\,\mathrm{d}t\right],\quad c\leqslant x\leqslant d \quad (56)$$

where

$$P(t)=-\zeta\frac{\left(\frac{f_6}{f_1}+\frac{f_8}{f_7}\right)\left(\frac{f_7}{f_4}\right)}{\left(\frac{f_6}{f_1}-\frac{f_5}{f_2}\right)\left(\frac{f_2}{f_3}\right)}\frac{\sqrt{e}}{e+t} \quad (57)$$

Eq. (56) can be reduced to

$$\phi(x)=[(x-c)(d-x)]^{-1/2}\left[B-\frac{\left(\frac{f_6}{f_1}+\frac{f_8}{f_7}\right)\left(\frac{f_7}{f_4}\right)}{\left(\frac{f_6}{f_1}-\frac{f_5}{f_2}\right)\left(\frac{f_2}{f_3}\right)}\frac{\sqrt{e}}{\alpha}+\frac{\left(\frac{f_6}{f_1}+\frac{f_8}{f_7}\right)\left(\frac{f_7}{f_4}\right)}{\left(\frac{f_6}{f_1}-\frac{f_5}{f_2}\right)\left(\frac{f_2}{f_3}\right)}\frac{\sqrt{e(c+e)(d+e)}}{\alpha(x+e)}\right],\quad c\leqslant x\leqslant d \quad (58)$$

The constant B in (58) is determined from the condition (55) on $\phi(x)$ as

$$B=\frac{\left(\frac{f_6}{f_1}+\frac{f_8}{f_7}\right)\left(\frac{f_7}{f_4}\right)}{\left(\frac{f_6}{f_1}-\frac{f_5}{f_2}\right)\left(\frac{f_2}{f_3}\right)}\frac{\sqrt{e}}{\alpha}\left[1-\sqrt{(c+e)(d+e)}\frac{\int_c^d\frac{\mathrm{d}t}{(t+e)\sqrt{t(t-c)(d-t)}}}{\int_c^d\frac{\mathrm{d}t}{\sqrt{t(t-c)(d-t)}}}\right] \quad (59)$$

The final form of $\phi(x)$ becomes

$$\phi(x)=\frac{\left(\frac{f_6}{f_1}+\frac{f_8}{f_7}\right)\left(\frac{f_7}{f_4}\right)}{\left(\frac{f_6}{f_1}-\frac{f_5}{f_2}\right)\left(\frac{f_2}{f_3}\right)}\frac{1}{\alpha}\sqrt{e(c+e)(d+e)}\left[\frac{1}{x+e}-\frac{1}{d+e}\frac{\Pi(k,m,\pi/2)}{K(k,\pi/2)}\right][(x-c)(d-x)]^{-1/2},\quad c\leqslant x\leqslant d \quad (60)$$

where

$$\Pi(k,m,\pi/2) = \int_0^{\pi/2} \frac{\mathrm{d}\theta}{(1+m\sin^2\theta)\sqrt{1-k^2\sin^2\theta}} \tag{61a}$$

$$K(k,\pi/2) = \int_0^{\pi/2} \frac{\mathrm{d}\theta}{\sqrt{1-k^2\sin^2\theta}} \tag{61b}$$

$$k^2 = \frac{d-c}{d}, \quad m = -\frac{d-c}{d+e} \tag{61c}$$

$K(k,\pi/2)$ and $\Pi(k,m,\pi/2)$ are the complete elliptic integrals of the first and third kinds respectively.

With the aid of (54), $f(r)$ is also obtained as the following closed-form (Shahani and Adibnazari, 2000):

$$f(r) = \frac{\left(\frac{f_6}{f_1}+\frac{f_8}{f_7}\right)\left(\frac{f_7}{f_4}\right)}{\left(\frac{f_6}{f_1}-\frac{f_5}{f_2}\right)\left(\frac{f_2}{f_3}\right)} \frac{1}{\alpha}\sqrt{h^{\zeta}(a^{\zeta}+h^{\zeta})(b^{\zeta}+h^{\zeta})}\left[\frac{1}{r^{\zeta}+h^{\zeta}} - \frac{1}{b^{\zeta}+h^{\zeta}}\frac{\Pi(k,m,\pi/2)}{K(k,\pi/2)}\right]\left(r^{(\zeta/2)-1}\right) \times \frac{1}{\sqrt{(r^{\zeta}-a^{\zeta})(b^{\zeta}-r^{\zeta})}}, \quad a \leqslant r \leqslant b \tag{62}$$

where

$$k^2 = \frac{b^{\zeta}-a^{\zeta}}{b^{\zeta}}, \quad m = -\frac{b^{\zeta}-a^{\zeta}}{b^{\zeta}+h^{\zeta}} \tag{63}$$

From (29) and (52), the function $g(r)$ can be obtained in a similar way as follows

$$g(r) = \frac{\left(\frac{f_5}{f_2}+\frac{f_8}{f_7}\right)\left(\frac{f_7}{f_4}\right)}{\left(\frac{f_6}{f_1}-\frac{f_5}{f_2}\right)\left(\frac{f_1}{f_3}\right)} \frac{1}{\alpha}\sqrt{h^{\zeta}(a^{\zeta}+h^{\zeta})(b^{\zeta}+h^{\zeta})}\left[\frac{1}{r^{\zeta}+h^{\zeta}} - \frac{1}{b^{\zeta}+h^{\zeta}}\frac{\Pi(k,m,\pi/2)}{K(k,\pi/2)}\right]\left(r^{(\zeta/2)-1}\right) \times \frac{1}{\sqrt{(r^{\zeta}-a^{\zeta})(b^{\zeta}-r^{\zeta})}}, \quad a \leqslant r \leqslant b \tag{64}$$

The relationship of functions $f(r)$ and $g(r)$ can be shown as

$$g(r) = \frac{\left(\frac{f_5}{f_2}+\frac{f_8}{f_7}\right)f_2}{\left(\frac{f_6}{f_1}+\frac{f_8}{f_7}\right)f_1} f(r) \tag{65}$$

3.3. Stresses, strains, electric displacements and electric fields

In the region $a \leqslant r \leqslant b$ of material 1, the stresses and electric displacements are obtained by substituting (44) and (45) into (10)–(11) respectively:

$$\sigma_{\theta z}^{(1)}(r,\theta) = \frac{F}{r}[-X_1 - X_2 + X_3], \quad a \leqslant r \leqslant b \tag{66a}$$

$$D_{\theta}^{(1)}(r,\theta) = \frac{Q}{r}[-X_1 - X_2 + X_3], \quad a \leqslant r \leqslant b \tag{66b}$$

where

$$X_1 = \frac{2}{\pi}\sum_{n=1}^{\infty}\frac{(-1)^n}{2n-1}\left(\frac{r}{h}\right)^{p_n} p_n \cos(p_n\theta) \tag{67a}$$

$$X_2 = -\sum_{n=1}^{\infty}\frac{\left(\int_a^r \left(\frac{v}{r}\right)^{p_n} f^*(v)\,\mathrm{d}v\right)\sin(p_n\theta - p_n\alpha)}{\alpha\sin(p_n\alpha)} \tag{67b}$$

$$X_3 = -\sum_{n=1}^{\infty}\frac{\left(\int_r^b \left(\frac{v}{r}\right)^{-p_n} f^*(v)\,\mathrm{d}v\right)\sin(p_n\theta - p_n\alpha)}{\alpha\sin(p_n\alpha)} \tag{67c}$$

and

$$f(r) = \frac{\left(\frac{f_6}{f_1}+\frac{f_8}{f_7}\right)\left(\frac{f_7}{f_4}\right)}{\left(\frac{f_6}{f_1}-\frac{f_5}{f_2}\right)\left(\frac{f_2}{f_3}\right)} f^*(r) \tag{68}$$

From (62), we see that function $f^*(r)$ is independent of material properties. Using the constitutive equation (1), we can obtain the relationships

$$\gamma_{\theta z}^{(1)} = \frac{D_\theta^{(1)} e_{15}^{(1)} + \sigma_{\theta z}^{(1)} \varepsilon_{11}^{(1)}}{e_{15}^{(1)^2} + c_{44}^{(1)} \varepsilon_{11}^{(1)}} \tag{69a}$$

$$E_\theta^{(1)} = \frac{D_\theta^{(1)} c_{44}^{(1)} - \sigma_{\theta z}^{(1)} e_{15}^{(1)}}{e_{15}^{(1)^2} + c_{44}^{(1)} \varepsilon_{11}^{(1)}} \tag{69b}$$

Substituting (66) into (69), the strains and electric fields in $a \leqslant r \leqslant b$ of material 1 can be obtained, respectively.

It is noticed that the stress field is independent of material properties and electric charge Q. Meanwhile, the electric displacement field is independent of material properties and mechanical load F. This conclusion is true when the following conditions are satisfied: (1) These two wedge angles are equal; (2) A pair of equal longitudinal shear forces is applied at same distance; (3) Two equal electric charges are applied at same distance.

The same conclusion was met in our previous study (Wei et al., 2002) for the same bimaterial piezoelectric wedge without considering the interface crack. In this case the stress and electric displacement for $r \leqslant h$ are as follows (Wei et al., 2002):

$$\sigma_{\theta z}^{(1)}(r,\theta) = \sigma_{\theta z}^{(2)}(r,\theta) = \frac{F}{r\alpha}\left[\frac{h^{\frac{\pi}{2\alpha}} r^{\frac{\pi}{2\alpha}} (h^{\frac{\pi}{\alpha}} + r^{\frac{\pi}{\alpha}})\cos\frac{\pi\theta}{2\alpha}}{h^{\frac{2\pi}{\alpha}} + r^{\frac{2\pi}{\alpha}} + 2h^{\frac{\pi}{\alpha}} r^{\frac{\pi}{\alpha}}\cos\frac{\pi\theta}{\alpha}}\right] \tag{70a}$$

$$D_\theta^{(1)}(r,\theta) = D_\theta^{(2)}(r,\theta) = \frac{Q}{r\alpha}\left[\frac{h^{\frac{\pi}{2\alpha}} r^{\frac{\pi}{2\alpha}} (h^{\frac{\pi}{\alpha}} + r^{\frac{\pi}{\alpha}})\cos\frac{\pi\theta}{2\alpha}}{h^{\frac{2\pi}{\alpha}} + r^{\frac{2\pi}{\alpha}} + 2h^{\frac{\pi}{\alpha}} r^{\frac{\pi}{\alpha}}\cos\frac{\pi\theta}{\alpha}}\right] \tag{70b}$$

When we set $a = b$ in (66), the results are identical to (70). In the past, the results of several studies for antiplane interface crack problems (Chen et al., 1997; Li and Fan, 2001) and bimaterial elastic wedge problems with equal wedge angles (Erdogan and Gupta, 1975; Ma and Hour, 1989; Shahani and Adibnazari, 2000) also show that the stress field is independent of material properties.

3.4. Intensity factors at interface crack tips

Eq. (66) show that the stress and electric displacement are uncoupled and independent of material properties. Therefore, we define the stress and electric displacement intensity factors at the interface crack tips ($r = a$ and $r = b$) as follows (Erdogan and Gupta, 1975; Shahani and Adibnazari, 2000):

$$K^{\sigma}_{\mathrm{III}}(a) = \lim_{r\to a+} \sqrt{2\pi(r-a)}Ff^*(r) \tag{71a}$$

$$K^{\sigma}_{\mathrm{III}}(b) = -\lim_{r\to b-} \sqrt{2\pi(b-r)}Ff^*(r) \tag{71b}$$

$$K^{D}_{\mathrm{III}}(a) = \lim_{r\to a+} \sqrt{2\pi(r-a)}Qf^*(r) \tag{72a}$$

$$K^{D}_{\mathrm{III}}(b) = -\lim_{r\to b-} \sqrt{2\pi(b-r)}Qf^*(r) \tag{72b}$$

From the constitutive equation (1), the strain and electric field intensity factors become

$$K^{\gamma(i)}_{\mathrm{III}}(a) = \frac{Qe^{(i)}_{15} + F\varepsilon^{(i)}_{11}}{e^{(i)^2}_{15} + c^{(i)}_{44}\varepsilon^{(i)}_{11}} \lim_{r\to a+} \sqrt{2\pi(r-a)}f^*(r) \tag{73a}$$

$$K^{\gamma(i)}_{\mathrm{III}}(b) = -\frac{Qe^{(i)}_{15} + F\varepsilon^{(i)}_{11}}{e^{(i)^2}_{15} + c^{(i)}_{44}\varepsilon^{(i)}_{11}} \lim_{r\to b-} \sqrt{2\pi(b-r)}f^*(r) \tag{73b}$$

$$K^{E(i)}_{\mathrm{III}}(a) = \frac{Qc^{(i)}_{44} - Fe^{(i)}_{15}}{e^{(i)^2}_{15} + c^{(i)}_{44}\varepsilon^{(i)}_{11}} \lim_{r\to a+} \sqrt{2\pi(r-a)}f^*(r) \tag{73c}$$

$$K^{E(i)}_{\mathrm{III}}(b) = -\frac{Qc^{(i)}_{44} - Fe^{(i)}_{15}}{e^{(i)^2}_{15} + c^{(i)}_{44}\varepsilon^{(i)}_{11}} \lim_{r\to b-} \sqrt{2\pi(b-r)}f^*(r) \tag{73d}$$

where $i = 1, 2$ for materials 1 or 2. Eq. (73) show the coupling behaviors between mechanical and electric effects.

The asymptotic behaviors of $f^*(r)$ as r approaches a and b are important for obtaining intensity factors in (71)–(73). Fig. 2 plots the variation of function $f^*(r)$ from $r = a = 0.01$ m to $r = b = 0.02$ m when $\alpha = \pi/2$, and $h = 0.03$ m. There are two singularities at crack tips. This function can be used to get the relative crack opening displacement via Eq. (62), i.e.,

$$w^{(1)}(r,+0) - w^{(2)}(r,-0) = \int_a^r f(v)\,\mathrm{d}v, \quad a \leqslant r \leqslant b \tag{74}$$

According to previous works (Erdogan and Gupta, 1975; Shahani and Adibnazari, 2000), the function $f^*(r)$ can be shown as

$$f^*(r) = F^*(a^{\zeta})\frac{1}{\sqrt{\zeta a(b^{\zeta} - a^{\zeta})}}\frac{1}{\sqrt{(r-a)}}[1 + \mathrm{O}(r-a)], \quad 0 < (r-a) \ll (b-a) \tag{75a}$$

$$f^*(r) = F^*(b^{\zeta})\frac{1}{\sqrt{\zeta b(b^{\zeta} - a^{\zeta})}}\frac{1}{\sqrt{(b-r)}}[1 + \mathrm{O}(b-r)], \quad 0 < (b-r) \ll (b-a) \tag{75b}$$

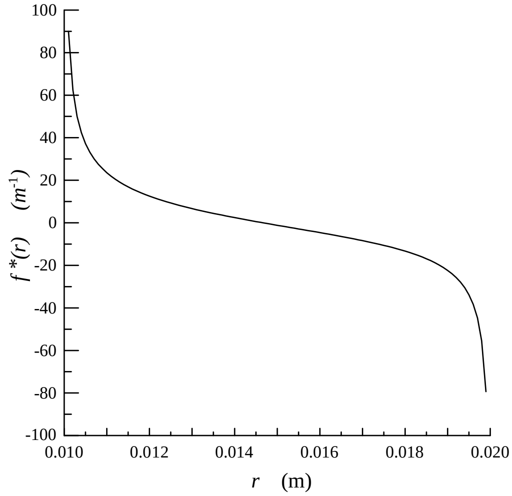

Fig. 2. Variations of function $f^*(r)$ with r for $a = 0.01$ m, $b = 0.02$ m, $h = 0.03$ m and $\alpha = \pi/2$.

where

$$F^*(r^\zeta) = \frac{1}{\alpha}\sqrt{h^\zeta(a^\zeta + h^\zeta)(b^\zeta + h^\zeta)}\left[\frac{1}{r^\zeta + h^\zeta} - \frac{1}{b^\zeta + h^\zeta}\frac{\Pi(k, m, \pi/2)}{K(k, \pi/2)}\right], \quad a \leqslant r \leqslant b \tag{76}$$

The higher order terms in (75) will not affect the intensity factors and can be ignored.

3.5. Energy density theory

It is known that simply considering the stress intensity factor by itself is not sufficient to explain the fracture behavior in piezoelectric materials. For studying the crack problem, two criteria are commonly employed: energy release rate criterion and energy density theory (Shen and Nishioka, 2000; Zuo and Sih, 2000; Soh et al., 2001). Lin et al. (2003) compared the results yielded by these two criteria for a piezoelectric layered composite with a permeable and impermeable crack normal to interface. In the impermeable case, when a larger electric field is applied either in a positive or negative direction, the total potential energy release rate decreases and eventually arrests the crack growth. However, experimental investigation has not confirmed this crack-arresting behavior (Park and Sun, 1995; Shindo et al., 2002).

The energy density $\frac{dW}{dV}$ near the crack tip under antiplane mechanical loads and inplane electric loads can be expressed by

$$\frac{dW}{dV} = \frac{S}{r_1} = \frac{1}{2}(\sigma_{r_1z_1}\gamma_{r_1z_1} + \sigma_{\theta_1z_1}\gamma_{\theta_1z_1} + D_{r_1}E_{r_1} + D_{\theta_1}E_{\theta_1}) \tag{77}$$

where (r_1, θ_1) is the localized coordinate system at crack tip B shown in Fig. 1. The near-field quantities near the interface crack tip B can be expressed as (Pak, 1990)

$$\sigma_{r_1z_1} = \frac{K^\sigma_{\mathrm{III}}}{\sqrt{2\pi r_1}}\sin\frac{\theta_1}{2} \tag{78}$$

$$\sigma_{\theta_1z_1} = \frac{K^\sigma_{\mathrm{III}}}{\sqrt{2\pi r_1}}\cos\frac{\theta_1}{2} \tag{79}$$

$$\gamma^{(i)}_{r_1z_1} = \frac{K^{\gamma(i)}_{\mathrm{III}}}{\sqrt{2\pi r_1}}\sin\frac{\theta_1}{2} \tag{80}$$

$$\gamma^{(i)}_{\theta_1 z_1} = \frac{K^{\gamma(i)}_{\mathrm{III}}}{\sqrt{2\pi r_1}} \cos\frac{\theta_1}{2} \tag{81}$$

$$D_{r_1} = \frac{K^{D}_{\mathrm{III}}}{\sqrt{2\pi r_1}} \sin\frac{\theta_1}{2} \tag{82}$$

$$D_{\theta_1} = \frac{K^{D}_{\mathrm{III}}}{\sqrt{2\pi r_1}} \cos\frac{\theta_1}{2} \tag{83}$$

$$E^{(i)}_{r_1} = \frac{K^{E(i)}_{\mathrm{III}}}{\sqrt{2\pi r_1}} \sin\frac{\theta_1}{2} \tag{84}$$

$$E^{(i)}_{\theta_1} = \frac{K^{E(i)}_{\mathrm{III}}}{\sqrt{2\pi r_1}} \cos\frac{\theta_1}{2} \tag{85}$$

where i is for materials 1 or 2. Substituting (78)–(85) into (77), we obtain

$$\left(\frac{\mathrm{d}W}{\mathrm{d}V}\right)^{(i)} = \frac{S^{(i)}}{r_1} = \frac{1}{4\pi r_1}\left[K^{\sigma}_{\mathrm{III}} K^{\gamma(i)}_{\mathrm{III}} + K^{D}_{\mathrm{III}} K^{E(i)}_{\mathrm{III}}\right] \tag{86}$$

or

$$S^{(i)} = \frac{1}{4\pi}\left[K^{\sigma}_{\mathrm{III}} K^{\gamma(i)}_{\mathrm{III}} + K^{D}_{\mathrm{III}} K^{E(i)}_{\mathrm{III}}\right] \tag{87}$$

Note that the energy density factors $S^{(i)}$ are independent of θ_1 in materials 1 or 2.

In the previous study, Sih (1973) discussed the Mode III crack propagation of isotropic media by using the strain energy density factor $S = a_{33}k_3^2$. S is independent of θ, an angle measured counterclockwise from crack surface (x-axis). Chen and Chue (2003) found the same conclusions for Mode III crack propagation in piezoelectric media.

4. Results and discussions

The effects of the wedge angle, interface crack location and crack length on the stress and electric displacement intensity factors are discussed in the following section. Due to similar forms of stress intensity factor $K^{\sigma}_{\mathrm{III}}$ and electric displacement intensity factor K^{D}_{III}, we use K^* to replace $K^{\sigma}_{\mathrm{III}}/F$ and K^{D}_{III}/Q. Two typical piezoelectric ceramics PZT-4 and PZT-5H are considered to show the variations of intensity factors around crack tips A and B. The material properties are $c_{44} = 2.56 \times 10^{10}$ N/m^2, $e_{15} = 12.7$ C/m^2, $\varepsilon_{11} = 64.6 \times 10^{-10}$ C/Vm for PZT-4 and $c_{44} = 2.3 \times 10^{10}$ N/m^2, $e_{15} = 17$ C/m^2, $\varepsilon_{11} = 150.4 \times 10^{-10}$ C/Vm for PZT-5H.

4.1. Effects of wedge angle

Fig. 3 plots the variations of $K^*(a)$ and $K^*(b)$ with wedge angle α for crack length $(b - a) = 0.01$ m and 0.005 m when $a = 0.01$ m and $h = 0.03$ m. The wedge angles (defined as α_C) with equal intensity factors of crack tips A and B are 0.37π and 0.40π for crack length 0.01 m and 0.005 m, respectively. It is observed that $K^*(a) > K^*(b)$ for $\alpha > \alpha_C$ and $K^*(a)$ reaches its maximum when $\alpha = \alpha_C$. However, when $\alpha < \alpha_C$, the intensity factor $K^*(b)$ reaches its maximum and is greater than $K^*(a)$.

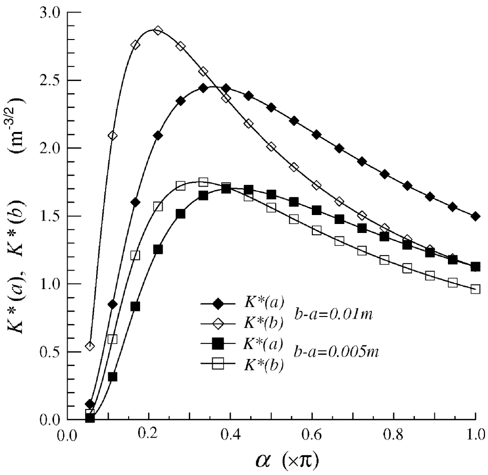

Fig. 3. Variation of the intensity factors $K^*(a)$ and $K^*(b)$ with α at different crack length $(b-a)$ when $a = 0.01$ m and $h = 0.03$ m.

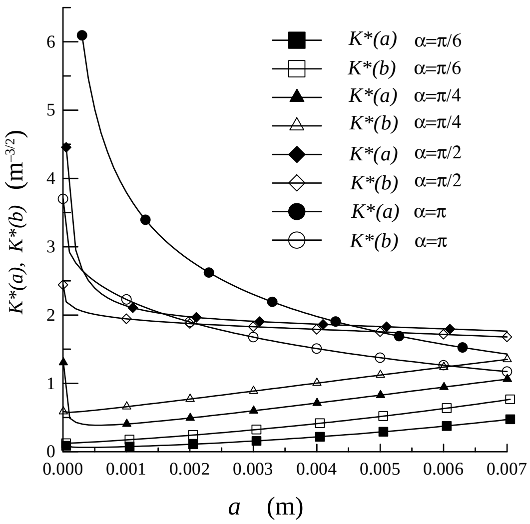

Fig. 4. Variation of the intensity factors $K^*(a)$ and $K^*(b)$ with a at different wedge angle when $b-a = 0.005$ m and $h = 0.03$ m.

4.2. Effects of interface crack location

Consider the case of crack length 0.005 m and $h = 0.03$ m. From the previous section, we know that $\alpha_C = 0.40\pi$. Fig. 4 shows the variations of $K^*(a)$ and $K^*(b)$ with distance $r = a$. Intensity factors $K^*(a)$ and $K^*(b)$ decrease for larger distance a when the wedge angle (such as $\alpha = \pi/2$, π) is greater than α_C. On the contrary, the intensity factors increase for larger a when $\alpha < \alpha_C$. It also can be seen that $K^*(a)$ is unbounded if the crack tip (point A) approaches the wedge apex.

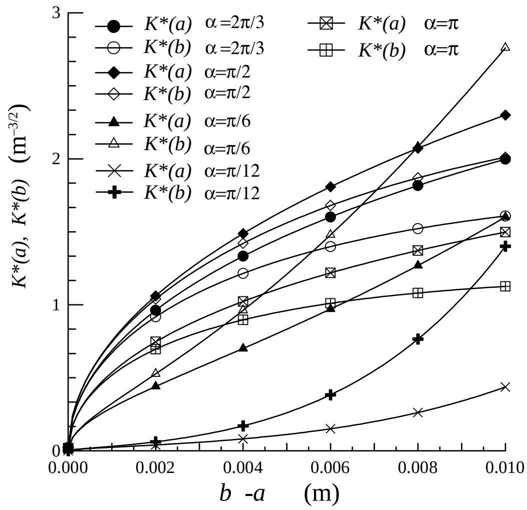

Fig. 5. Variation of the intensity factors $K^*(a)$ and $K^*(b)$ with crack length $(b-a)$ at different wedge angle when $a = 0.01$ m and $h = 0.03$ m.

4.3. Effects of interface crack length

Under the conditions of $a = 0.01$ m and $h = 0.03$ m, Fig. 5 plots the distributions of intensity factors with crack length $(b-a)$ at different wedge angle α. The results show that $K^*(a)$ and $K^*(b)$ increase for longer crack length.

References

Chen, C.D., Chue, C.H., 2003. Fracture mechanics analysis of a composite piezoelectric strip with an internal semi-infinite electrode. Theoretical and Applied Fracture Mechanics 39, 291–314.

Chen, Z.T., Yu, S.W., Karihaloo, B.L., 1997. Antiplane shear problem for a crack between two dissimilar piezoelectric materials. International Journal of Fracture 86, L9–L12.

Chen, Z.T., Worswick, M.J., 2000. Antiplane mechanical and inplane electric time-dependent load applied to two coplanar cracks in piezoelectric ceramic. Theoretical and Applied Fracture Mechanics 33, 173–184.

Chue, C.H., Liu, C.I., 2001. A general solution on stress singularities in an anisotropic wedge. International Journal of Solids and Structures 38, 6889–6906.

Chue, C.H., Chen, C.D., 2002. Decoupled formulation of piezoelectric elasticity under generalized plane deformation and its application to wedge problems. International Journal of Solids and Structures 39, 3131–3158.

Chue, C.H., Chen, C.D., 2003. Antiplane stress singularities in a bimaterial piezoelectric wedge. Archive of Applied Mechanics 72, 673–685.

Chue, C.H., Wei, W.B., Liu, T.J.C., 2003. The antiplane electro-mechanical field of a piezoelectric wedge under a pair of concentrated forces and free charges. Journal of the Chinese Institute of Engineers 26, 575–583.

Erdogan, F., Biricikoglu, V., 1973. Two bonded half planes with a crack going through the interface. International Journal of Engineering Science 11, 745–766.

Erdogan, F., Gupta, G.D., 1975. Bonded wedges with an interface crack under anti-plane shear loading. International Journal of Fracture 11, 583–593.

Kargarnovin, M.H., Shahani, A.R., Fariborz, S.J., 1997. Analysis of an isotropic finite wedge under antiplane deformation. International Journal of Solids and Structures 34, 113–128.

Li, X.F., Fan, T.Y., 2001. Mode-III interface edge crack between two bonded quarter-planes of dissimilar piezoelectric materials. Archive of Applied Mechanics 71, 703–714.

Lin, S., Narita, F., Shindo, Y., 2003. Comparison of energy release rate and energy density criteria for a piezoelectric layered composite with a permeable and impermeable crack normal to interface. Theoretical and Applied Fracture Mechanics 39, 229–243.

Ma, C.C., Hour, B.L., 1989. Analysis of dissimilar anisotropic wedges subjected to antiplane shear deformation. International Journal of Solids and Structures 11, 1295–1309.

Muskhelishvili, N.I., 1953. Singular Integral Equations. P. Noordhoff, Groningen, The Netherlands.

Pak, Y.E., 1990. Crack extension force in a piezoelectric material. ASME Journal of Applied Mechanics 57, 647–653.

Park, S.B., Sun, C.T., 1995. Fracture criteria for piezoelectric ceramics. Journal of the American Ceramic Society 78, 1475–1480.

Schneider, G.A., Felten, F., McMeeking, R.M., 2003. The electrical potential difference across cracks in PZT measured by Kelvin probe microscopy and the implications for fracture. Acta Materialia 51, 2235–2241.

Shahani, A.R., 1999. Analysis of an anisotropic finite wedge under antiplane deformation. Journal of Elasticity 56, 17–32.

Shahani, A.R., Adibnazari, S., 2000. Analysis of perfectly bonded wedges and bonded wedges with an interface crack under antiplane shear loading. International Journal of Solids and Structures 37, 2639–2650.

Shahani, A.R., 2001. A note on the paper ''Analysis of perfectly bonded wedges and bonded wedges with an interface crack under antiplane shear loading''. International Journal of Solids and Structures 38, 5041–5043.

Shen, S., Nishioka, T., 2000. Fracture of piezoelectric materials: energy density criterion. Theoretical and Applied Fracture Mechanics 33, 57–65.

Shindo, Y., Murakami, H., Hiriguchi, K., Narita, F., 2002. Evaluation of electric fracture properties of piezoelectric ceramics using the finite element and single-edge precracked-beam methods. Journal of the American Ceramic Society 85, 1243–1248.

Sih, G.C., 1973. In: Sih, G.C. (Ed.), Methods of Analysis and Solutions of Crack Problems. Martinus Nijhoff, The Netherlands.

Sneddon, I.N., 1972. The Use of Integral Transforms. McGraw-Hill, New York.

Soh, A.K., Fang, D.N., Lee, K.L., 2001. Fracture analysis of piezoelectric materials with defects using energy density theory. International Journal of Solids and Structures 38, 8331–8344.

Wei, W.B., Liu, T.J.C., Chue, C.H., 2002. Antiplane electro-mechanical field of a two-piezoelectric wedge under a pair of concentrated forces and free charges. The 26th National Conference on Theoretical and Applied Mechanics, Hu-Wei, Taiwan, ROC.

Xu, X.L., Rajapakse, R.K.N.D., 2000. On singularities in composite piezoelectric wedges and junctions. International Journal of Solids and Structures 37, 3253–3275.

Zhang, T.Y., Tong, P., 1996. Fracture mechanics for a mode III crack in a piezoelectric material. International Journal of Solids and Structures 33, 343–359.

Zhang, T.Y., Zhao, M.H., Tong, P., 2002. Fracture of piezoelectric ceramics. Advances in Applied Mechanics 38, 148–289.

Zuo, J.Z., Sih, G.C., 2000. Energy density theory formulation and interpretation of cracking behavior for piezoelectric ceramics. Theoretical and Applied Fracture Mechanics 34, 17–33.